Modeling the Solubility Behavior of CO_2, H_2, and Xe in [C_n-mim][Tf_2N] Ionic Liquids

Jordi S. Andreu[†,‡] **and Lourdes F. Vega***[,†,‡,§]

Consejo Superior de Investigaciones Científicas (ICMAB-CSIC), Institut de Ciència de Materials de Barcelona, Campus de la UAB, 08193 Bellaterra, Barcelona, Spain, MATGAS, Campus de la UAB, 08193 Bellaterra, Barcelona, Spain, and Carburos Metálicos—Air Products Group, C/Aragón 300, Barcelona, Spain

Received: August 21, 2008; Revised Manuscript Received: September 21, 2008

We present here a new model for the imidazolium-based ionic liquids (ILs) with the bis(trifluoromethylsulfonyl)imide anion $[Tf_2N]^-$ in the context of the *soft*-SAFT EoS. The model is used to predict the solubility of several compounds in these ILs, and results are compared to available experimental data. Since in the *soft*-SAFT EoS an associating site is used to represent a short-range and highly directional attractive force among molecules, we have used this feature to mimic the main interactions between the anion and the cation for the alkylimidazolium−[Tf_2N] ILs. The members of the alkylimidazolium−[Tf_2N] family are modeled as Lennard-Jones chains with three associating sites in each molecule (one "A" site and two "B" sites). An "A" site represents the nitrogen atom interactions with the cation, and a "B" site represents the delocalized charge due the oxygen molecules on the anion. Each type of associating site is identically defined, but only AB interactions between different IL molecules are allowed. Model parameters for the ionic liquids were estimated with experimental density data from different authors, following a similar approach taken in our previous work [Andreu and Vega, *J. Phys. Chem. C* **2007**, *111*, 16028]. The new set of parameters was used to study the solubility behavior of hydrogen, carbon dioxide, and xenon in these ILs over a wide range of temperature and pressure. It has been observed that no binary parameters are needed to correlate the solubility of hydrogen in [C_6-mim][Tf_2N] at different temperatures, and predictions up to 100 MPa are presented here. The model is able to correlate with very good agreement the experimental data for the systems [C_n-mim][Tf_2N] + CO_2 with only one temperature-independent mixture parameter, while two temperature-independent mixture parameters are needed to correlate the experimental solubility data for the systems IL + Xe, attaining an excellent agreement in a wide range of temperatures. The work presented here reinforces previous results, proving that a reasonable simple model for the IL within the framework of *soft*-SAFT is able to describe the physical absorption of different gases in ILs with good accuracy, in spite of the most complex nature of the anion, without the need of further parameters or terms. In addition, since these parameters do not depend on the particular conditions at which they were fitted, *soft*-SAFT is used then to analyze the solubility dependence of these gases in ILs, according to the anion nature and the alkyl chain length of the imidazolium cation by the use of the models developed within this approach.

1. Introduction

Ionic liquids (ILs) are usually defined as organic salts composed of large asymmetric organic cations and organic or inorganic anions with a melting point at or below 100 °C. They tend to have extremely low vapor pressure, good thermal stability, low melting point, high ionic conductivity, and large electrochemical window. The great interest about ILs in different areas of applied chemistry is that their properties can be tuned with a judicious selection of the cation−anion pair, giving the opportunity to select among a vast range of different ILs. In addition, ILs can also be tuned by the modification of the cation and/or the anion molecular structure using appropriate functional groups with the aim to obtain ILs with a set of desired physicochemical properties, designed for specific applications, which are known as task specific ionic liquids (TSILs). At the present time, hundreds of ILs have been synthesized, and there is virtually no limit in the number of possible counterions pairs and mixtures of them that can be obtained. For this reason, a good understanding about the dependence of their physicochemical properties on their microscopic structure and theoretical predictive tools are desired in order to enhance the design of new ILs for promising chemical and industrial processes.

A deeper understanding on the relation of their molecular structure and thermodynamic properties such as density, solubility, vapor−liquid equilibria (VLE), liquid−liquid equilibria (LLE), selectivity, and so on is needed before selecting them for specific applications. A considerable number of experimental and theoretical studies characterizing these substances have been done trying to understand the dependence of their thermodynamic and transport properties from a microscopic point of view. Latest experimental studies and molecular simulations based on the alkylimidazolium series of ILs have been focused on the anion−cation interactions,[1] the nanostructural organization,[2] and the different conformations of the anion and cation in the liquid phase and crystalline structure.[3−5] These achievements have offered new insights into the complex nature of such compounds at different thermodynamic conditions and their role in different systems. However, given the amount of potential

* Corresponding author: e-mail vegal@matgas.com, phone +34 935 929 950, fax +34 935 929 951.
† Institut de Ciència de Materials de Barcelona.
‡ MATGAS.
§ Carburos Metálicos—Air Products Group.

10.1021/jp807484g CCC: $40.75
Published on Web 11/06/2008

ionic liquids, there is still much work needed to characterize them before used in specific applications.

Their tunable and unique properties make them a good alternative to conventional volatile organic compounds (VOCs) used in reaction and separation processes, solvents for cleaning and purification operations, and as electrolytes in fuel cells, lubricants, heat transfer fluids, and storage media.[6−8] Specifically, understanding gas solubility in ionic liquids has became an important issue for several applications, like supercritical fluid extraction[9] and gas separations in supported ionic liquid membranes, alternative to the conventional amine scrubbing operation.[10] Clearly, an accurate knowledge of the phase behavior of these (gas + IL) systems is necessary in order to effectively design optimal ILs for these particular applications. An excellent manner to obtain the phase behavior of these systems is by modeling techniques, provided accurate models are available for this.

In this respect, different thermodynamic models and EoSs have been tested during the past years. The nonrandom two liquid model (NRTL) has been successfully applied to correlate different binary systems with ILs. Shiflett and Yokozeki[11] studied binary liquid−liquid equilibria of five hydrofluoroethers with [C_2-mim][Tf_2N], and Domańska and Marciniak have correlated LLE and SLE of imidazolium-based ILs with alcohols, water, ketones, and hydrocarbons.[12] Yang et al.[13] have successfully correlated infinite diluted activity coefficients, vapor pressures of solvents, and liquid−liquid equilibria of ILs solutions with a modified lattice model, which takes into account the hydrogen bonding through an exchange energy function. Good achievements were also obtained within the COSMO-RS model. Banarjee et al.[14] predicted the VLE for several alkylimidazolium-based ILs with the $[Tf_2N]^-$ anion and with acetone, 2-propanol, water, benzene, and cyclohexane with reasonable agreement. Nebig et al.[15] have used the modified UNIFAC (Dortmund) to correlate the VLE of different binary systems with several alkylimidazolium ILs with the $[Tf_2N]^-$ anion. They have also used the equation to calculate the excess enthalpies and to predict the activity coefficients at infinite dilution.

In the framework of equations of state (EoSs), some attempts trying to model the solubility of gases in ionic liquids have been done at different thermodynamic conditions by different authors. These works have mainly focused in some of the most widely studied families of ILs: the alkylimidazolium cation with $[BF_4]^-$ and $[PF_6]^-$ anions. Wang and co-workers[16] have used a square-well chainlike fluid EoS (SWCF-EoS) to correlate the solubility of carbon dioxide, propane, propene, and butane (CO_2, C_3H_8, C_3H_6, and C_4H_{10}) in [C_n-mim][BF_4] and [C_n-mim][PF_6] ILs up to 15 MPa, obtaining a good agreement using two temperature-dependent interaction parameters. Karakatsani and co-workers[17] have reparametrized their previous model with the tPC-PSAFT EoS fitting IL density data over a wide temperature range and restricting the model to predict very low vapor pressure values, according to recent experimental results.[18] Breure et al.[19] have used a group contribution equation of state (GC-EoS) to predict the phase behavior of binary systems of ionic liquids ([C_n-mim][BF_4] and [C_n-mim][PF_6]) with carbon dioxide up to 40 MPa with good agreement and with a reasonable agreement up to 100 MPa. Recently, Yokozeki and Shiflett[6] have used a generic Redlich−Kwong (RK) type of cubic EoS to study the ternary system CO_2/H_2/[C_4-mim][PF_6]. They correlated the solubility data of CO_2/[C_4-mim][PF_6] and H_2/[C_4-mim][PF_6] systems in order to obtain the selectivity of those compounds at different feed compositions.

Moreover, the combination of alkylimidazolium cation with the bis(trifluoromethylsulfonyl)imide anion $[Tf_2N]^-$ has attracted the attention of most recent studies on gas absorption due to the high solubility exhibited by several gases in these ILs by simple physical absorption. In addition, these ILs are highly hydrophobic and exhibit low viscosities and high thermal and electrochemical stability, which make them suitable candidates for industrial applications.

Some attempts to model the solubility of gases in ILs with the $[Tf_2N]^-$ anion have also been done recently within the framework of equations of state. Kim et al.[20] have applied a group contribution nonrandom lattice fluid (GC-NLF EoS) to correlate the solubility of carbon dioxide and propane in [C_6-mim][Tf_2N] and also ternary systems CO_2/N_2/[C_6-mim][Tf_2N] and CO_2/propane/[C_6-mim][Tf_2N] at $T = 298$ K and up to 1 MPa with reasonable agreement. Wang and co-workers[21] have studied the VLE of several binary systems containing imidazolium-based ILs using an equation of state for the heteronuclear square-well chain fluids (hetero-SWCF). They modeled the ILs as "diblock compounds": the alkyl group as one block and the imidazolium ring and anion as the other block with a reasonable agreement with experimental data. Shiflett and Yokozeki[22] have correlated the solubility of CO_2 in [C_6-mim][Tf_2N] up to 2 MPa with a Redlich−Kwong EoS (RK-EoS) and in a temperature range between 282 and 348 K, in agreement with their experimental measurements.

In our previous work[23] a simple model for the alkylimidazolium-based ILs with the $[BF_4]^-$ and $[PF_6]^-$ anions was proposed and used to describe the behavior of these ILs as compared to experimental data. The ILs were modeled as a one molecule (cation and anion bound together) with one associating site in each molecule mimicking the attraction between counterions belonging to different ion pairs. After fitting the model parameters to experimental density data, we correlated carbon dioxide solubility data at low pressure. The binary parameters obtained from the correlations were used to predict the behavior of those systems at different thermodynamic conditions. We showed that this model suffices to capture the solubility behavior of carbon dioxide in those ILs up to 90 MPa, over a wide range of temperatures, without any specific interaction between the ILs and the carbon dioxide, and using only one mixture parameter, temperature independent, for each family of ILs.

The approach we followed in this work is similar to the previous one.[23] In this case, the more complex nature on the anion is taken into account by including new specific interactions in the model, keeping the same number of parameters as for the alkylimidazolium family with $[BF_4]^-$ and $[PF_6]^-$ anions. A molecular model for the ILs is developed here, and parameters are fitted to available experimental data, providing a correlation of the molecular parameters with the molecular weight of the ILs. Before fitting any binary data, molecular parameters from the pure compounds are used to check if the model is able to capture the behavior of the mixture. As stated, this is possible thanks to the manner in which SAFT equations are constructed. Empirical and semiempirical models, like traditional cubic equations of state, have limited predictive capabilities, particularly outside the range where their parameters were fitted. Parameters of a molecular model based on statistical mechanics have physical meaning and are independent of the thermodynamic conditions. Furthermore, an important advantage of using molecular based theories vs mean-field approaches is that the first one can consider intramolecular and intermolecular interactions among the molecules, as the model is based on the molecular structure of the components.

The rest of the paper is organized as follows: we briefly outline the *soft*-SAFT equation and the molecular models used in the next sections, followed by results and discussion. Finally, some concluding remarks are provided in the last section.

2. *soft*-SAFT Modeling

The *soft*-SAFT EoS was proposed by Blas and Vega in 1997.[24] It is a modification of the original SAFT proposed by Chapman et al.[25] and Huang and Radosz,[26] being the main difference the term used for the reference fluid. As all SAFT-type equations, the chain and association terms come from a first-order perturbation theory (TPT1) based on Wertheim's work.[27,28] Since SAFT equations have been widely revised during the past years, we just retain here the main features relevant for this work. The reader is referred to two reviews on the subject[29,30] and to ref 31 for details.

SAFT equations are usually written in terms of the residual Helmholtz energy. Each term in the equation represents different microscopic contributions to the total free energy of the fluid. According to the models used in this work, the residual Helmholtz energy is written as

$$a^{\mathrm{res}} = a^{\mathrm{ref}} + a^{\mathrm{chain}} + a^{\mathrm{assoc}} + a^{\mathrm{polar}} \tag{1}$$

where a^{res} is the residual Helmholtz free energy density of the system ($a^{\mathrm{res}} = a^{\mathrm{total}} - a^{\mathrm{ideal}}$). The superscripts ref, chain, assoc, and polar refer to the contributions from the reference term, the formation of the chain, the association, and the polar interactions, respectively. The use of these different terms depends on the particular system under study, according to its physical nature.

In the *soft*-SAFT EoS,[24,32,33] the reference term is a Lennard-Jones (LJ) spherical fluid, which accounts for both the repulsive and attractive interactions of the monomers forming the chain. As in previous works, the accurate EoS of Johnson et al.[34] is used here to calculate the reference term. For the case of mixtures the same equation is used by applying the van der Waals one-fluid theory, with generalized Lorentz−Berthelot mixing rules:

$$\sigma_{ij} = \eta_{ij}\left(\frac{\sigma_{ii} + \sigma_{jj}}{2}\right) \tag{2}$$

$$\varepsilon_{ij} = \xi_{ij}(\varepsilon_{ii}\varepsilon_{jj})^{1/2} \tag{3}$$

where η and ξ are the size and energy binary adjustable parameters for the species i and j, respectively. The equation is used in a purely predictive manner from the pure component parameters when η and ξ are equal to unity, while values different from unity mean the use of one or two binary parameters, taking into account the differences in size and/or energy of the segments forming the two compounds in the mixture, respectively. Note that the ξ parameter is equivalent to $(1 - k)$ in most EoSs.

The chain and association terms come from Wertheim's theory, and they are formally identical in the different versions of SAFT—only differing in the reference fluid model used in each version. In the case of the *soft*-SAFT the reference model is a LJ fluid.

$$a^{\mathrm{chain}} = \rho k_{\mathrm{B}} T \sum_i x_i (1 - m_i) \ln g_{\mathrm{LJ}}(\sigma_{ii}) \tag{4}$$

where ρ is the molecular density, T is the temperature, x_i is the molar fraction of component i, k_{B} is the Boltzmann constant, and g_{LJ} is the radial distribution function of a fluid of LJ spheres at density $\rho_m = m\rho$, evaluated at the bond length σ_{ii}.

The association term is expressed as the sum of the contributions of all associating sites of component i:

$$a^{\mathrm{assoc}} = \rho k_{\mathrm{B}} T \sum_i x_i \sum_{\alpha} \left(\ln X_i^{\alpha} - \frac{X_i^{\alpha}}{2}\right) + \frac{M_i}{2} \tag{5}$$

where M_i is the number of associating sites of component i and X_i^{α} is the mole fraction of molecules of component i nonbonded at site α, which accounts for the contributions of all the associating sites in each species.

The leading multipolar term for fluids of linear symmetrical molecules, like carbon dioxide, nitrogen, acetylene, etc., is the quadrupole−quadrupole potential.[35] An expansion of the Helmholtz free energy density in terms of the perturbed quadrupole−quadrupole potential with the Padé approximation was proposed by Stell et al.:[36]

$$a^{qq} = a_2^{qq}\left(1 - \frac{a_3^{qq}}{a_2^{qq}}\right)^{-1} \tag{6}$$

a_2^{qq} and a_3^{qq}, the second- and third-order perturbation terms, were derived for an arbitrary intermolecular reference potential[37,38] and involve the state variables, molecular parameters, and the integral J for the reference fluid. A detailed derivation of these expressions is given elsewhere.[35]

This term in the *soft*-SAFT EoS involves an additional molecular parameter, Q, the quadrupolar moment. The inclusion of this term has been demonstrated to be crucial in molecules with important quadrupolar interactions, like carbon dioxide.[39]

3. Molecular Models

The development of a molecular model for the pure compounds is a necessary step before any calculation can be done with *soft*-SAFT. We present here the *soft*-SAFT models used for the pure compounds, for the different gases, and for the ionic liquids.

The models used for xenon, hydrogen, and carbon dioxide have already been used in previous works,[39−41] leading to accurate and contrasted results, while the model for the alkylimidazolium−[Tf_2N] series of ILs is presented for the first time here.

Xenon was modeled[41] as a spherical LJ molecule with two characteristic parameters: σ, the diameter of the spheres, and ε, the energy of interaction between the different spheres. Hydrogen was modeled[40] as LJ chains, with three molecular parameters: m, the chain length, σ, the diameter of the spheres forming the chain, and ε, the energy of interaction between the different spheres forming the molecule. These parameters were obtained by fitting the equation to the vapor−liquid equilibrium experimental data.[42]

The carbon dioxide molecule was modeled[39] as a LJ chain in which explicit quadrupolar interactions were taken into account. In this case, the molecule was represented by five molecular parameters: m, the chain length, σ, the segment

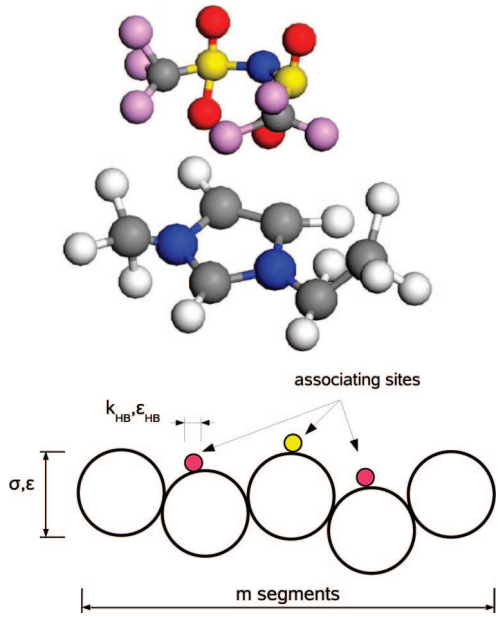

Figure 1. Sketch of the model used to describe the [C_n-mim][Tf_2N] family of ILs within the *soft*-SAFT approach. See text for details.

TABLE 1: Optimized Molecular Parameters for the Gases Used in This Work[a]

	M_w [g mol^{-1}]	m	σ [Å]	ε/k_B [K]	Q [C m^2]	ref
H_2	2.016	0.4874	4.244	33.85		40
CO_2	44.01	1.571	3.184	160.2	4.4×10^{-40}	39
Xe	131.29	1.000	3.953	226.6		41

[a] For further details see references corresponding to the works in which the models were developed.

size, ε, the energy parameter of the segments making the chain and those related to the quadrupolar interactions: the quadrupolar moment Q and x_p, defined as the fraction of segments in the chain that contain the quadrupole. The value for the quadrupole moment Q for this molecule obtained from the fitting is in agreement with the ones present in the literature.[43,44] The value of x_p was fixed to 1/3, thus mimicking the molecule as three segments with a quadrupole in one of them. Therefore, with x_p and Q fixed, only the usual m, σ, and ε parameters needed to be adjusted. This model has already been used with success to describe the behavior of CO_2 on different systems.

According to experimental and theoretical studies, using EoSs to describe systems with ILs can be justified due the evidence that anions and cations are associated together, forming ionic pairs or ionic clusters[45,46] in the bulk fluid state. Besides, the bulky size and the asymmetric charge distribution of molecular ions soften the Coulomb forces and generate highly directional interactions of shorter range.[47] This fact justifies the use of specific associating sites in order to mimic the strong interactions between counterions. According to those assumptions and due to the scarce experimental thermodynamic data available for these compounds, as a first step, we have used a very crude model of the ionic liquids within the *soft*-SAFT approach, sketched in Figure 1. Since in the *soft*-SAFT EoS an associating site is used to represent a short-range and highly directional attractive force among molecules, we used this feature to mimic the main interactions between the anion and the cation for the alkylimidazolium−[Tf_2N] ILs. The main interaction between counterions is due to the Coulombic forces as a consequence

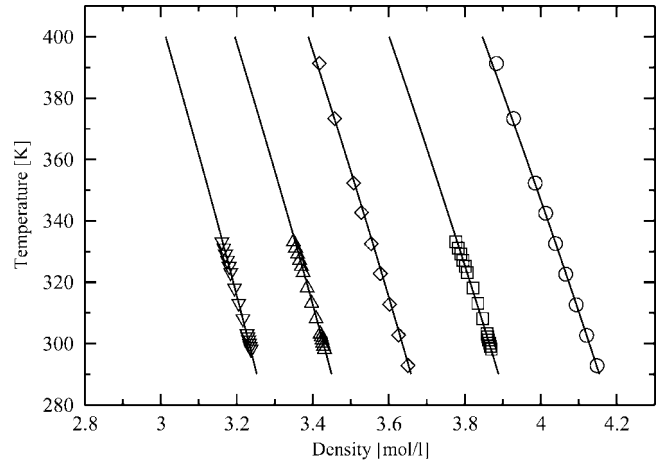

Figure 2. Temperature−density diagram for the [C_2-mim][Tf_2N] (circles), [C_3-mim][Tf_2N] (squares), [C_4-mim][Tf_2N] (diamonds), [C_5-mim][Tf_2N] (triangle up), and [C_6-mim][Tf_2N] (triangle down) used in the molecular parameters fitting procedure. Symbols are experimental data,[48−50] and solid lines are the *soft*-SAFT estimation.

of their opposite electric charge. Moreover, the delocalization of the anion electric charge due to the oxygen groups enhances the possibility of interaction with the surrounding cations through them. Hence, the members of the alkylimidazolium−[Tf_2N] family are modeled as LJ chains with three associating sites in each molecule (let us say one "A" site and two "B" sites). According to these interactions, we used an "A" site representing the nitrogen atom interactions with the cation and a "B" site representing the delocalized charge due the oxygen molecules on the anion. Each type of associating site is identically defined, but only AB interactions between different IL molecules are allowed, according to the modeled specific interactions on such systems. Five molecular parameters were used to characterize these compounds: m, the chain length, σ, the diameter of the spheres forming the chain, ε, the energy of interaction between them, k_{HB}, the volume of association, and ε_{HB}, the association energy. The values of the association parameters were used from previous work on the imidazolium−[BF_4] and imidazolium−[PF_6] families in order to avoid further fitting of parameters, searching for the transferability of the new model. The rest of molecular parameters were obtained by fitting to selected experimental data from the literature. In some preliminary work (not shown here) we also tried a two site model (instead of the three site model presented here), and results were not as accurate as the ones presented next. Hence, the number of chosen sites has an influence on the accuracy of the final results. However, it should be noted that *soft*-SAFT is a thermodynamic perturbation theory of first order (TPT1); consequently, the equation is not able to distinguish among different locations of the sites.

4. Results and Discussion

A. Pure Components. As we stated in the previous section, a needed step before applying the equation to mixtures is to obtain the molecular parameters of the pure compounds. The set of *soft*-SAFT parameters for carbon dioxide, hydrogen, and xenon is presented in Table 1 for completeness.

As for the ILs, m, σ, and ε were obtained by fitting to selected experimental density data from the literature, while the association parameters were used from previous work. Among the available data in the literature, we have chosen those provided in refs 48−50. The choice was based on the extended temper-

TABLE 2: Optimized Molecular Parameters for the [C_n-mim][Tf_2N] Series[a]

	M_w [g mol^{-1}]	M	σ [Å]	ε/k_B [K]	k_{HB} [Å^3]	ε_{HB}/k_B [K]	ref
[C_2-mim][Tf_2N]	367.29	5.660	4.050	365.0	2250	3450	48
[C_3-mim][Tf_2N]	381.31	5.740	4.122	367.0	2250	3450	49
[C_4-mim][Tf_2N]	395.34	5.810	4.191	369.0	2250	3450	48
[C_5-mim][Tf_2N]	409.36	5.896	4.254	370.5	2250	3450	49
[C_6-mim][Tf_2N]	423.39	5.995	4.315	372.0	2250	3450	50
[C_8-mim][Tf_2N]	451.44	6.151	4.427	375.37	2250	3450	

[a] Parameters for the members from $n = 2$ to $n = 6$ were obtained from fitting. Parameters corresponding to the [C_8-mim][Tf_2N] have been obtained using the correlations presented in eqs 7−9. See text for details. References correspond to the experimental data used in the fitting.

ature range investigated and also because of their agreement with other published data. Results for the temperature density diagram are shown in Figure 2 while the parameters are provided in Table 2. The density AAD for this series of ILs is less than 0.4%. As obtained in previous work for similar systems, three of the molecular parameters for the alkylimidazolium−[Tf_2N] family correlate with the molecular weight, while the other two (those related to association) are kept constant for the whole family. None of these parameters are temperature dependent.

$$m = 0.0059M_w + 3.4919 \quad (7)$$

$$m\sigma^3\ (\text{Å}^3) = 1.877M_w - 313.670 \quad (8)$$

$$m\varepsilon/k_B\ (\text{K}) = 2.898M_w - 1000.700 \quad (9)$$

These correlations enable the equation with predictive power, as they provide the possibility to predict the behavior of heavier members of the series, not included in the fitting procedure, offering the possibility of studying compounds for which few or none solubility data have been reported.

Once the models for the pure compounds were set up, we used them to predict the solubility behavior of hydrogen, carbon dioxide, and xenon in the imidazolium−[Tf_2N] family of ILs, and the results concerning the application of the model and parameters to available data for those gases with selected members of ILs family are presented and discussed next.

B. Solubility of H_2 in [C_6-mim][Tf_2N]. First we notice that, as known from experimental data, the hydrogen absorption depends on temperature, but in this case, the absorption increases with increasing temperature. *Soft*-SAFT predictions also capture this trend, as it was expected, given the performance of the model for similar systems.[40]

Results concerning calculations for the system [C_6-mim][Tf_2N] + H_2 at three different temperatures within the *soft*-SAFT approach are presented in Figure 3. An excellent agreement with the experimental data available for that system[56] is found. It should be remarked that this quantitative agreement is obtained *without the need of binary parameters*; these are predictions from pure component parameters. Using this predictive power, we have calculated the solubility isotherms of hydrogen in [C_6-mim][Tf_2N] up to 100 MPa, at three different temperatures, and results are presented in Figure 4, showing that hydrogen is poorly absorbed in this IL even at very high pressures.

C. Solubility of CO_2 in [C_n-mim][Tf_2N]. The solubility of CO_2 in the ILs [C_2-mim][Tf_2N], [C_4-mim][Tf_2N], and [C_6-mim][Tf_2N] over a wide temperature range (313−453 K) was calculated with *soft*-SAFT, and results are compared to available experimental data.[22,51,53−55] Calculations from pure component parameters (no mixture parameters adjusted) are able to capture

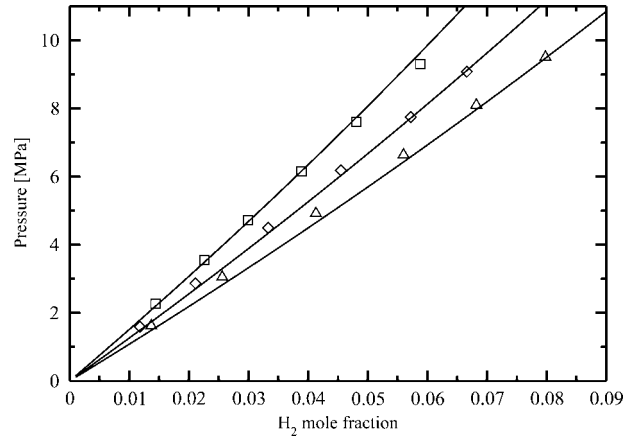

Figure 3. Pure prediction of the H_2 solubility in [C_6-mim][Tf_2N] at three different temperatures: $T = 333$ K (squares), $T = 373$ K (diamonds), and $T = 413$ K (triangles) and low pressure. In this case no binary parameters were needed to fit the isotherms. Experimental data from ref 56.

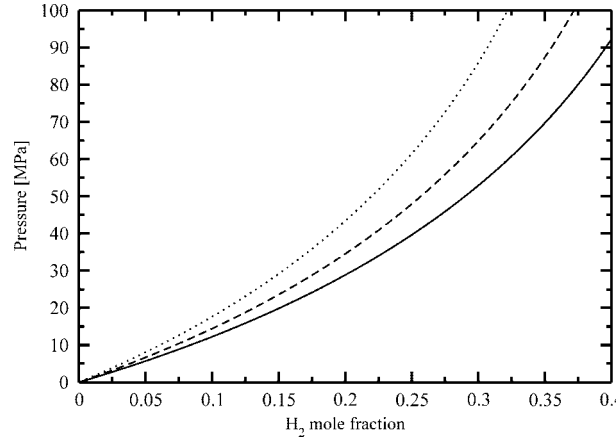

Figure 4. Predicted solubility of H_2 in [C_6-mim][Tf_2N] (no fitting) at three different temperatures: $T = 333$ K (dotted line), $T = 373$ K (dashed line), and $T = 413$ K (solid line) up to 100 MPa.

the behavior of the system at high pressure, but deviations from experimental data are found. As we can see in Figure 5 (inset), the solubility of CO_2 in the three members of the family is overpredicted when pure component parameters are used. Results were improved by using one binary parameter, independent of temperature. For this purpose we fitted the solubility isotherms for CO_2 at low pressure (up to 15 MPa for the [C_2-mim]$^+$ cation, 8 MPa for the [C_4-mim]$^+$ cation, and up to 4 MPa for the [C_6-mim]$^+$ cation). This approach is the same taken in our previous work for the alkylimidazolium-based ILs with [BF_4]$^-$ and [PF_6]$^-$ anions,[23] but different values according to the alkyl chain length of the imidazolium ring are required in the present case ($\xi = 0.985$, 0.972, and 0.948 for $n = 2$, 4, and 6, respectively). A good qualitative agreement with experimental data is found for all ILs is obtained, as depicted in Figure 5.

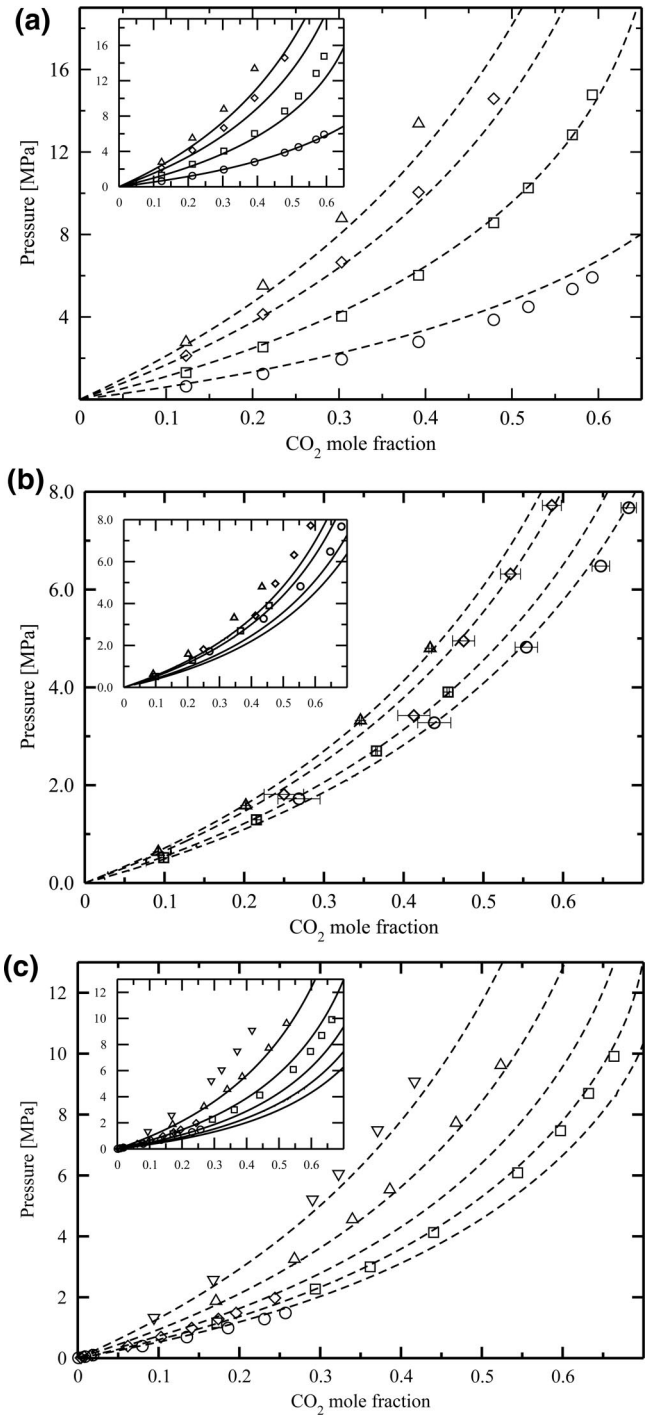

Figure 5. (a) Predicted solubility of CO_2 in [C_2-mim][Tf_2N] at four different temperatures: $T = 313.15$ K (circles), $T = 363.15$ K (squares), $T = 413.15$ K (diamonds), and $T = 473.15$ K (triangles). Solid lines are the *soft*-SAFT pure predictions (no binary parameter fitted), and dashed lines are the *soft*-SAFT calculations with a temperature-independent parameter $\xi = 0.985$. (b) Solubility of CO_2 in [C_4-mim][Tf_2N] at four different temperatures: $T = 313.3$ K (circles), $T = 320$ K (squares), $T = 333.3$ K (diamonds), and $T = 340$ K (triangles). Solid lines are pure predictions. Dashed lines are the *soft*-SAFT calculations with a temperature independent parameter $\xi = 0.972$. (c) Solubility of CO_2 in [C_6-mim][Tf_2N] at five different temperatures: $T = 322.9$ K (circles), $T = 333.15$ K (squares), $T = 348.5$ K (diamonds), $T = 373.2$ K (triangles up), and $T = 413.2$ K (triangles down). Solid lines are pure predictions, and dashed lines correspond to calculations with $\xi = 0.948$. Experimental data from refs 22, 51, and 53−55.

We notice that a better fit for $n = 6$ was obtained when using two different values of the binary parameter, a value of 0.940 for $T = 322.9$ K and $T = 348$ K, and a value of $\xi = 0.958$ for the three highest temperatures (not shown here). Results presented in Figure 5 for $n = 6$ were obtained with an intermediate value of $\xi = 0.948$. This seems to indicate some discrepancies on the solubility of carbon dioxide in the IL [C_6-mim][Tf_2N] between the experimental data reported by two different groups, at different temperatures. The calculated solubility of carbon dioxide in this ILs at $T = 322.9$ K and $T = 348.5$ K[54] when using with $\xi = 0.948$ is slightly overpredicted compared to the experimental data, while is underpredicted for the other three isotherms ($T = 333.15$, 373.20, and 413.20 K).[22] Note that the three isotherms at high temperature were measured using two different samples of this IL, leading to identical results, while in the low-temperature case only one set of compounds was used. The value of $\xi = 0.958$ used for the three highest temperatures follows the trend of the four chain lengths when using with ξ values, decreasing as the chain length of the alkyl chain increases (as shown below, the value required for the CO_2 + [C_8-mim][Tf_2N] is $\xi = 0.950$), enhancing the performance of the model and the consistency of the experimental data.

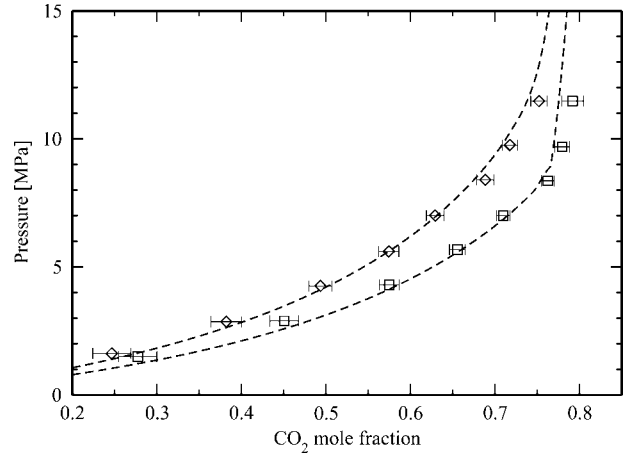

Figure 6. Solubility of CO_2 in [C_8-mim][Tf_2N] at two different temperatures: $T = 313.3$ K (squares) and $T = 333.3$ K (diamonds). Symbols are experimental data from ref 55. Dashed lines are *soft*-SAFT calculations with a binary parameter $\xi = 0.950$ for both isotherms. The molecular parameters for the [C_8-mim][Tf_2N] were obtained using the model correlations (eqs 7−9).

The results obtained with the *soft*-SAFT are in quantitative agreement with the experimental data available in the literature, and further experimental data at high pressure would be desired in order to check the model accuracy at higher pressures.

Experimental data for the solubility of CO_2 in [C_8-mim][Tf_2N] are available,[55] although no experimental density−temperature data for the pure IL have been published. Hence, using the correlations presented previously for this model (eqs 7−9), we set up the *soft*-SAFT parameters for the [C_8-mim][Tf_2N] compound (Table 2). With those parameters we have calculated the absorption of CO_2 in this IL, and the results have been compared with experimental data from ref 55. In this case, we adjusted the binary parameter ($\xi = 0.950$) according to the alkyl chain length dependence observed for the lower compounds. The predicted parameters for this compound based on the correlations, eqs 7−9, lead to a good agreement with experimental solubility data available at two different temperatures, as shown in Figure 6.

D. Solubility of Xenon in [C_6-mim][Tf_2N]. The solubility results for the system [C_6-mim][Tf_2N] + Xe within the range $T = 333$−413 K are presented next. Calculations with pure

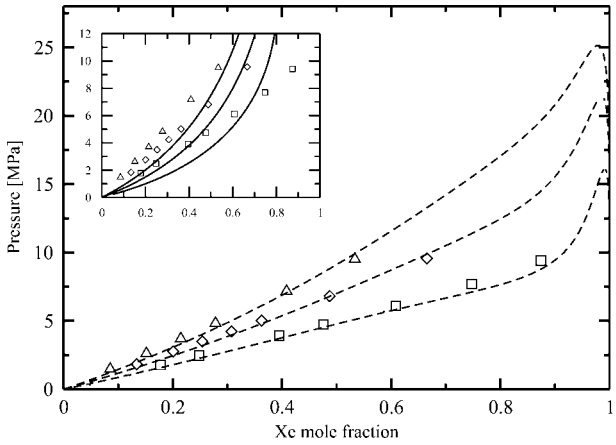

Figure 7. Solubility of Xe in [C_6-mim][Tf_2N] at three different temperatures: $T = 333$ K (squares), $T = 373$ K (diamonds), and $T = 413$ K (triangles). Symbols are experimental data.[57] Dashed lines are calculations with $\xi = 0.990$ and $\xi = 1.080$ for all solubility isotherms. The inset shows *soft*-SAFT predictions with no binary parameters (solid lines), with the same set of experimental data.

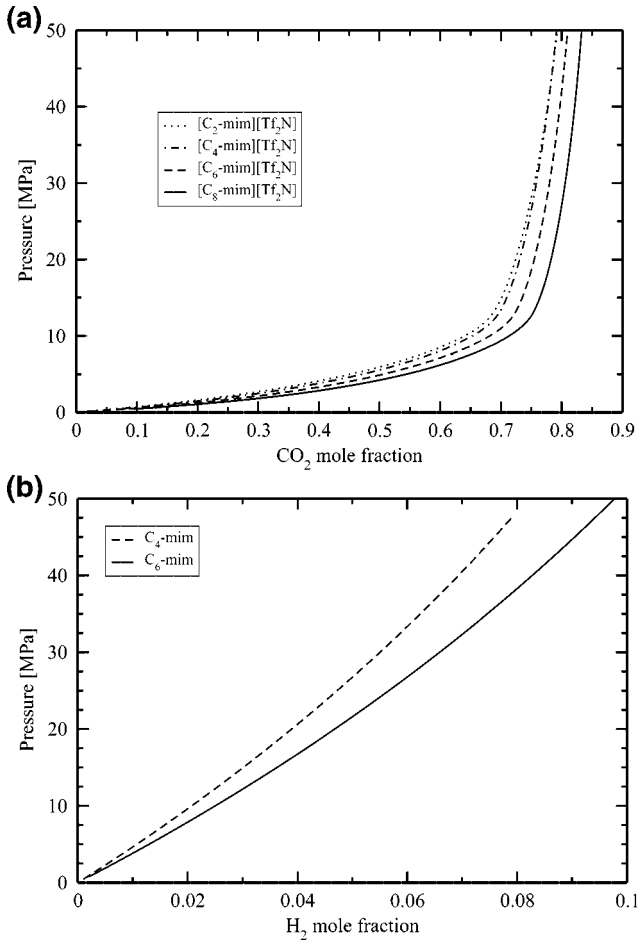

Figure 8. (a) Solubility of CO_2 in [C_n-mim][Tf_2N] for $n = 2$ (dotted), $n = 4$ (dashed-dotted), $n = 6$ (dashed), and $n = 8$ (solid) at $T = 333.3$ K using the optimized parameters. The solubility of CO_2 increases as the chain length of the imidazolium cation increases. (b) Solubility of H_2 in [C_n-mim][PF_6] at $T = 333$ K for $n = 4$ and 6. The same behavior as for the carbon dioxide is found in this case.

component parameters were performed first and results compared with experimental data,[57] as shown in the inset of Figure 7. The solubility of xenon is overestimated at all temperatures and low pressure if no binary parameters are used. The best fit for those mixtures was obtained using two binary parameters:

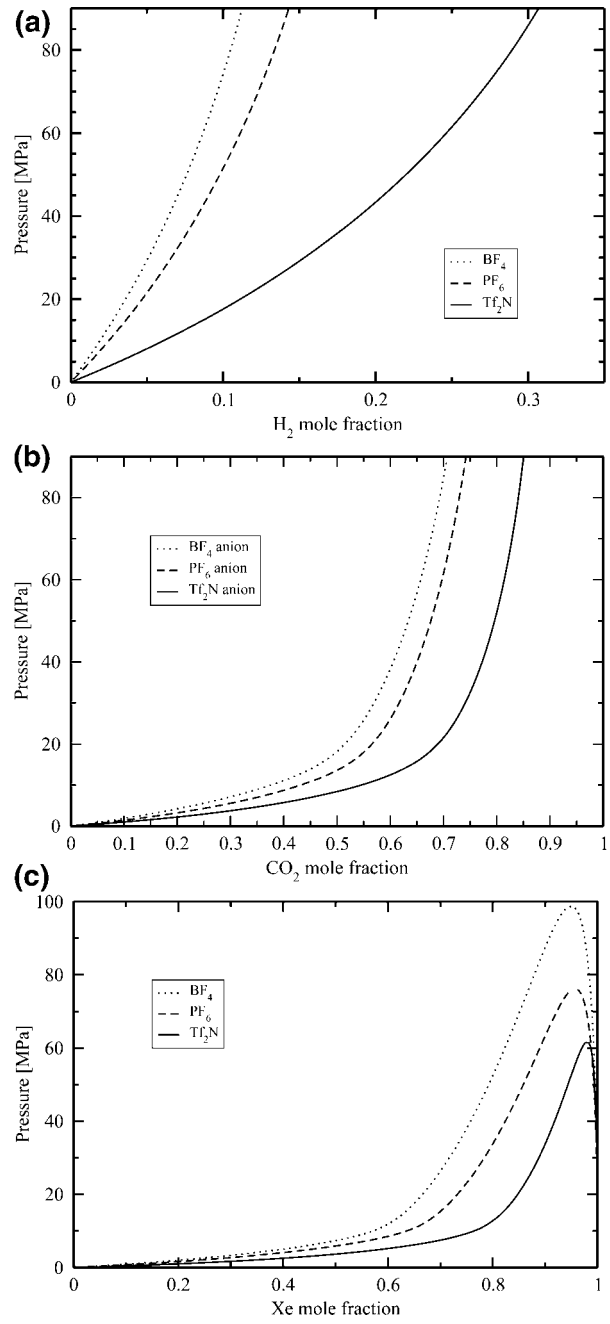

Figure 9. Comparison of the solubility of H_2, CO_2, and Xe in 1-alkyl-3-methylimidazolium-based ILs with three different anions. (a) [C_n-mim][X] + H_2 at $T = 333.15$ K. (b) [C_n-mim][X] + CO_2 at $T = 363.15$ K. (c) [C_n-mim][X] + Xe at $T = 333.15$ K. The $[Tf_2N]^-$ anion (solid line) shows the highest solubility capacity for all gases, followed by the $[PF_6]^-$ anion (dashed line) and the $[BF_4]^-$ anion (dotted line).

the usual energy mixture parameter ($\xi = 0.990$) and the volume mixture parameter ($\eta = 1.080$), both of them close to unity. As depicted in Figure 7, excellent results were obtained in this case.

E. Solubility Dependence Analysis. Taking advantage of the predictive and extrapolative power of the equation, pure predictions for IL + gas systems were performed in order to analyze the solubility behavior as a function of the molecular structure. We present here two different comparisons on the solubility of H_2, CO_2, and Xe in alkylimidazolium-based ILs.

First, the influence of the alkyl chain length of the cation is checked by comparing the solubility of CO_2 and H_2 in different members of the [C_n-mim][Tf_2N] and the [C_n-mim][PF_6] family, respectively. Figure 8a shows results concerning the system [C_n-

mim][Tf_2N] + CO_2 at $T = 333.3$ K for $n = 2$, 4, 6, and 8, while Figure 8b depicts the ones corresponding to the [C_n-mim][PF_6] + H_2 system at $T = 333$ K for $n = 4$ and 6. We observe that a higher absorption capability of carbon dioxide and hydrogen is found in these ILs when increasing the chain length of the imidazolium cation.

Second, the influence of the anion on the solubility of different gases was also investigated. For this purpose, different calculations with the three different anions, $[BF_4]^-$, $[PF_6]^-$, and $[Tf_2N]^-$, and the same cation were done. We calculated the solubility of hydrogen, carbon dioxide, and xenon in ILs with same cation but different anion. The results concerning these three systems ([C_6-mim][X] + H_2 at $T = 333.15$ K, [C_2-mim][X] + CO_2 at $T = 363.15$ K, and [C_6-mim][X] + Xe at $T = 333.15$ K) are presented in Figure 9. In all cases the $[Tf_2N]^-$ anion exhibits the highest absorption capability for these gases, followed by the $[PF_6]^-$ and the $[BF_4]^-$ anions.

5. Conclusions

A new simple model for alkylimidazolium−[Tf_2N] ILs within the context of *soft*-SAFT has been presented here. The model has been used to check the capability of *soft*-SAFT in capturing the solubility of different gases in these ILs, and results are compared to available experimental data. We have shown that *soft*-SAFT captures the behavior of complex ILs with a simple approach, which enables the possibility to develop more refined and detailed models for more complex ILs, in a systematic manner. The solubility of hydrogen, carbon dioxide, and xenon in the imidazolium−[Tf_2N] family of ILs was accurately described without the need of explicit weak interactions.

The model was able to precisely reproduce the solubility of hydrogen at different temperatures, in a pure predictive manner, enabling the equation with predictive power at higher pressures, for which experimental data are not available. Only one binary interaction parameter, independent of temperature, suffices to describe the solubility of carbon dioxide in excellent agreement with experimental data. However, in the case of xenon, two temperature-independent parameters were needed to adequately describe the solubility data. No extra assumption on the interactions between the molecules in those binary systems was necessary to establish a predictive model for this family, showing that the solubility of gases in these ILs is due to physical absorption processes.

Finally, the models developed within this approach were used in order to analyze the solubility dependence on the alkyl chain length of the cation and on the anion nature, obtaining a description according to the experimental results: for the same anion, the solubility increases as the alkyl chain length of the cation increases, while for the same cation, the $[Tf_2N]^-$ anion exhibits the highest absorption capacity in all cases.

Acknowledgment. Discussions with Dr. Brian K. Peterson are gratefully acknowledged. Financial support has been provided by the Spanish Government, Ministerios de Educación y Ciencia y Ciencia e Innovación (projects CTQ2005-00296/PPQ and CTQ2008-05370/PPQ), Programa Ingenio 2010, CENIT SOST-CO2 CEN-2008-1027, and the Catalan Government (2005SGR-00288). J.S.A. acknowledges a grant from MATGAS 2000 AIE.

References and Notes

(1) Tsuzuki, S.; Tokuda, H.; Hayamizu, K.; Watanabe, M. *J. Phys. Chem. B* **2005**, *109*, 16474.
(2) Canongia Lopes, J. N. A.; Pádua, A. A. H. *J. Phys. Chem. B* **2006**, *110*, 3330.
(3) Umebayashi, Y.; Fujimori, T.; Sukizaki, T.; Asada, M.; Fujii, K.; Kanzaki, R.; Ishiguro, S. *J. Phys. Chem. A* **2005**, *109*, 8976.
(4) Fujii, K.; Fujimori, T.; Takamuku, T.; Kanzaki, R.; Umebayashi, Y.; Ishiguro, S. *J. Phys. Chem. B* **2006**, *110*, 8179.
(5) Lassègues, J. C.; Grondin, J.; Holomb, R.; Johansson, P. *J. Raman Spectrosc.* **2007**, *38*, 551.
(6) Yokozeki, A.; Shiflett, M. B. *Appl. Energy* **2007**, *84*, 351.
(7) Brennecke, J. F.; Maginn, E. J. *AIChE J.* **2001**, *47*, 2384.
(8) Temple, D. J.; Henderson, P. B.; Brzozowski, J. R.; Pearlstein, R. M.; Cheng, H. *J. Am. Chem. Soc.* **2008**, *130*, 400.
(9) Blanchard, L. A.; Brennecke, J. F. *Ind. Eng. Chem. Res.* **2001**, *40*, 287.
(10) Baltus, R. E.; Counce, R. M.; Culbertson, B. H.; Luo, H.; DePaoli, D. W.; Dai, S.; Duckworth, D. C. *Sep. Sci. Technol.* **2005**, *40*, 524.
(11) Shiflett, M. B.; Yokozeki, A. *J. Chem. Eng. Data* **2007**, *52*, 2413.
(12) Domańska, U.; Marciniak, A. *Fluid Phase Equilib.* **2007**, *260*, 9.
(13) Yang, J.; Peng, C.; Liu, H.; Hu, Y. *Ind. Eng. Chem. Res.* **2006**, *45*, 6811.
(14) Banerjee, T.; Singh, M. K.; Khanna, A. *Ind. Eng. Chem. Res.* **2006**, *45*, 3207.
(15) Nebig, S.; Bölts, R.; Gmehling, J. *Fluid Phase Equilib.* **2007**, *258*, 168.
(16) Wang, T.; Peng, C.; Liu, H.; Hu, Y. *Fluid Phase Equilib.* **2006**, *250*, 150.
(17) Karakatsani, E. K.; Economou, I. G.; Kroon, M. C.; Peters, C. J.; Witkamp, G. *J. Phys. Chem. C* **2007**, *111*, 15487.
(18) Zaitsau, D. H.; Kabo, G. J.; Strechan, A. A.; Paulechka, Y. U.; Tschersich, A.; Verevkin, S. P.; Heintz, A. *J. Phys. Chem. A* **2006**, *110*, 7303.
(19) Breure, B.; Bottini, S.; Witkamp, G.; Peters, C. J. *J. Phys. Chem. B* **2007**, *111*, 14265.
(20) Kim, Y. S.; Jang, J. H.; Lim, B. D.; Kang, J. W.; Lee, C. S. *Fluid Phase Equilib.* **2007**, *256*, 70.
(21) Wang, T.; Peng, C.; Liu, H.; Hu, Y.; Jiang, J. *Ind. Eng. Chem. Res.* **2007**, *46*, 4323.
(22) Shiflett, M. B.; Yokozeki, A. *J. Phys. Chem. B* **2007**, *111*, 2070.
(23) Andreu, J. S.; Vega, L. F. *J. Phys. Chem. C* **2007**, *111*, 16028.
(24) Blas, F. J.; Vega, L. F. *Mol. Phys.* **1997**, *92*, 135.
(25) Chapman, W. G.; Gubbins, K. E.; Jackson, G.; Radosz, M. *Fluid Phase Equilib.* **1989**, *52*, 31.
(26) Huang, S. H.; Radosz, M. *Ind. Eng. Chem. Res.* **1990**, *29*, 2284.
(27) Wertheim, M. S. *J. Stat. Phys.* **1984**, *35*, 19–35.
(28) Wertheim, M. S. *J. Stat. Phys.* **1986**, *42*, 459–477.
(29) Müller, E.; Gubbins, K. E. *Ind. Eng. Chem. Res.* **2001**, *40*, 2193.
(30) Economou, I. G. *Ind. Eng. Chem. Res.* **2002**, *41*, 953.
(31) Pàmies, J. C. PhD Thesis, Universitat Rovira i Virgili, Tarragona, Spain.
(32) Pàmies, J. C.; Vega, L. F. *Ind. Eng. Chem. Res.* **2001**, *40*, 2532.
(33) Blas, F. J.; Vega, L. F. *Ind. Eng. Chem. Res.* **1998**, *37*, 660.
(34) Johnson, J.; Zollweg, J.; Gubbins, K. *Mol. Phys.* **1993**, *78*, 591.
(35) Gubbins, K. E.; Two, C. H. *Chem. Eng. Sci.* **1978**, *33*, 863.
(36) Stell, G.; Rasaiah, J. C.; Narang, H. *Mol. Phys.* **1974**, *27*, 1393.
(37) Two, C. H.; Gubbins, K. E.; Gray, C. G. *Mol. Phys.* **1975**, *29*, 713.
(38) Two, C. H. PhD Dissertation, University of Florida, 1976.
(39) Dias, A. M. A.; Carrier, H.; Daridon, J. L.; Pàmies, J. C.; Vega, L. F.; Coutinho, J. A. P.; Marrucho, I. M. *Ind. Eng. Chem. Res.* **2006**, *45*, 2341.
(40) Florusse, L. J.; Peters, C. J.; Pàmies, J. C.; Vega, L. F.; Meijer, H. *AIChE J.* **2003**, *49*, 3260.
(41) Dias, A. M. A.; Pàmies, J. C.; Coutinho, J. A. P.; Marrucho, I. M.; Vega, L. F. *J. Phys. Chem. B* **2004**, *108*, 1450.
(42) Linstrom P. J., Mallard, W. G., Eds. NIST Chemistry WebBook, NIST Standard Reference Database Number 69, June 2005, National Institute of Standards and Technology, Gaithersburg MD, 20899 (http://webbook.nist.gov).
(43) Vravec, J.; Stoll, J.; Hasse, H. *J. Phys. Chem. B* **2001**, *105*, 12126.
(44) Vrbancich, J.; Ritchie, G. L. D. *J. Chem. Soc., Faraday Trans. 2* **1980**, *76*, 648.
(45) Marcus, Y.; Hefter, G. *Chem. Rev.* **2006**, *106*, 4585.
(46) Yokozeki, A.; Kasprzak, D. J.; Shiflett, M. B. *Phys. Chem. Chem. Phys.* **2007**, *9*, 5018.
(47) Weingärtner, H. *Angew. Chem., Int. Ed.* **2008**, *47*, 654.
(48) Jacquemin, J.; Husson, P.; Padua, A. A. H.; Majer, V. *Green Chem.* **2006**, *8*, 172.
(49) Esperança, J. M. S. S.; Visak, Z. P.; Plechkova, N. V.; Seddon, K. R.; Guedes, H. J. R.; Rebelo, L. P. N. *J. Chem. Eng. Data* **2006**, *51*, 2009.
(50) Gomes de Azevedo, R.; Esperança, J. M. S. S.; Szydlowski, J.; Visak, Z. P.; Pires, P. F.; Guedes, H. J. R.; Rebelo, L. P. N. *J. Chem. Thermodyn.* **2005**, *37*, 888.
(51) Zhao, D.; Liao, Y.; Zhang, Z. *Clean* **2007**, *35*, 42.

(52) Schilderman, A. M.; Raeissi, S.; Peters, C. J. *Fluid Phase Equilib.* **2007**, *260*, 19.
(53) Lee, B.; Outcalt, S. L. *J. Chem. Eng. Data* **2006**, *51*, 892.
(54) Kumelan, J.; Kamps, A. P.; Tuma, D.; Maurer, G. *J. Chem. Thermodyn.* **2006**, *38*, 1396.
(55) Aki, N.V.K.S.; Mellein, B. R.; Saurer, E. M.; Brennecke, J. F. *J. Phys. Chem. B* **2004**, *108*, 20355.
(56) Kumelan, J.; Kamps, A. P.; Tuma, D.; Maurer, G. *J. Phys. Eng. Data* **2006**, *51*, 1364.
(57) Kumelan, J.; Kamps, A. P.; Tuma, D.; Maurer, G. *Ind. Eng. Chem. Res.* **2007**, *46*, 8236.

JP807484G